Geotechnical Engineering

High-capacity ribbed pile foundations
Gorasia and McNamara

ice | proceedings

Proceedings of the Institution of Civil Engineers

http://dx.doi.org/10.1680/jgeen.15.00073
Paper 1500073
Received 09/04/2015 Accepted 19/11/2015
Keywords: geotechnical engineering/models (physical)/piles & piling

ice Institution of Civil Engineers
publishing

High-capacity ribbed pile foundations

1 Rohit Jay Gorasia MEng, PhD, CEng, MICE, FGS
Senior Engineer, BuroHappold, London, UK
(corresponding author: rohit@gorasia.net)

2 Andrew McNamara MSc, PhD
Senior Lecturer, City University London, London, UK

This research concerns the influence of ribs on the ultimate capacity of a bored pile in overconsolidated clay. Ribbed bored piles are known to give increased shaft capacity in comparison to conventional straight-shafted bored piles. The investigation seeks to explore the effectiveness of ribs at increasing the ultimate capacity of a pile, and furthermore to understand how this enhanced capacity is derived. The scale pile test results are analysed using several industry standard methods. A plastic failure envelope for the base of the pile rib is identified. This plastic failure envelope is used to provide a detailed design solution for the ultimate capacity of a ribbed pile. The design solution is simple and requires a summation of the constitutive contributions from each rib and from the base and shaft of the pile. This method has been used successfully to predict the ultimate capacity of any pile tested to within ±8%.

Notation

A_b	cross-sectional area of pile base
A_s	shaft area
F_{NU}	normalised ultimate failure load
K	percentage of longitudinal cross-sectional area compared to reference pile
K_0	coefficient of earth pressure at rest
L	pile length
M	percentage of capacity when compared to a reference pile
N_c	bearing capacity factor
Q_b	ultimate base resistance
Q_{rb}	ultimate base resistance from each rib
Q_{rs}	ultimate skin friction along rib shaft
Q_s	ultimate skin friction
Q_u	ultimate loading capacity of pile
$S_{u(avg)}$	average undrained shear strength of clay along pile shaft
$S_{u(base)}$	undrained shear strength at pile base
W	pile self-weight
α	adhesion factor
γ	unit weight of soil
ϕ'	angle of shearing resistance

1. Introduction

In urban areas developers aim to build increasingly tall structures in confined spaces. It is therefore necessary for foundations to carry larger loads. To accommodate greater loads engineers have no option but to bore deeper and wider piles, at closer spacing. Eventually, this becomes unfeasible.

Many modern buildings leave behind a set of deep foundations and the foundations for new buildings have to be installed through and between remnants of historic foundations (Qerimi, 2009). Geotechnical engineers therefore have an increasingly difficult task when finding locations for additional piles and providing sufficient capacity (Chapman *et al.*, 2001). The addition of slimmer ribbed piles can only help designers in this regard.

In 2002 Expanded Piling and Arup Geotechnics agreed to cooperate in a jointly funded programme of research consisting of a limited number of full-scale field trials, undertaken by Expanded Piling and supported by numerical analyses conducted by Arup Geotechnics. The field trials involved construction of several ribbed piles, which in turn required preliminary development work on a custom tool used for profiling the shaft. The analyses and tests yielded promising results and suggested that pile capacity could be increased by 30–40% (Ground Engineering, 2003).

The technique of providing a mechanically rough pile–soil interface with the use of ribs has demonstrated increased shaft capacity in the field, and has been confirmed by numerical analyses, but there is a need to test a wider range of geometries in various soil conditions to establish how the additional capacity that such piles offer is derived.

Given the obvious potential for commercial exploitation of ribbed piled foundations, an in-depth study of the factors affecting behaviour at the pile shaft–soil interface has been undertaken. This is in order to understand how increases in pile capacity can be optimised and, furthermore, to develop guidelines for the important factors affecting the design and construction of high-capacity piles.

2. Experimental design and procedure

An experimental approach has been developed for use in a geotechnical centrifuge that is capable of simultaneously loading one plain pile and one ribbed pile within a sample of overconsolidated clay, with a view to exploring the effect of these features on the ultimate capacities of the piles. Although the piles were loaded simultaneously, the apparatus was devised such that it was possible to obtain independent load and settlement data. The plain pile was tested to allow for normalisation and hence resolve any issues of inconsistencies between soil models.

In total, seven centrifuge tests were undertaken, in each of which two piles were tested. In all of the centrifuge tests one pile was always ribbed and the other plain. Once the model was installed into the centrifuge the sample was allowed to come into pore pressure equilibrium and the piles were then subjected to increasing load until 3 mm of settlement was measured. This is 15% of the maximum pile diameter and was chosen to ensure pile failure had been achieved. Once loading was complete, the undrained shear strength of the soil sample was profiled using a T-bar penetrometer. For each centrifuge test the pre-consolidation pressure, soil type, pile length and principal pile diameter were kept constant. Measurements of the pile settlement and the load applied were recorded.

3. Model geometry

Each test soil sample provided three testing sites within the soil container of 420 mm diameter. Two of the sites were used for piles and the third for the T-bar penetrometer. As the soil container was a cylindrical tub it was decided to locate each test site on a pitch circle diameter of 240 mm. This ensured that each site was sufficiently far away from the boundaries of the tub and from adjacent test sites to minimise any influence they may have had on each other. Craig (1995) suggests that for a pile foundation test, a minimum distance of five pile diameters from the boundaries is sufficient to minimise boundary effects. For the main series of tests using 16 mm diameter by 180 mm long piles, a spacing of at least 6·5 pile diameters was maintained between all boundaries. Furthermore, the sides of the soil container were lubricated with grease to minimise the skin friction at the boundaries. The pile length to diameter ratio is small when compared to typical piles used in the field; however, this was not considered to be problematic because the research aimed to develop a better fundamental understanding of ribbed piles.

4. Soil used and stress history

The clay samples for the tests were prepared from slurry at a water content of approximately 120% which, for speswhite kaolin, is twice the liquid limit. Mixing of the dry kaolin powder and distilled water was conducted using an industrial ribbon blade mixer.

The soil container was prepared by coating the walls with water pump grease. The slurry was then sandwiched between a layer of filter paper and 3 mm porous plastic, at either end, in combination with the aluminium drainage plate. This arrangement was found to provide an effective drainage system, which also prevented the loss of clay slurry during the early stages of consolidation. Since the required slurry height (600 mm) was much greater than the height available in the soil container (300 mm), an extension was required.

Although the slurry was at a water content of 120% post mixing it was still too viscous to be poured into the soil container without the use of special equipment. It was therefore carefully placed using a scoop and spatula to prevent the entrapment of air. Once the slurry had been placed and levelled the top filter paper and porous plastic were positioned to enable top drainage. A hydraulic consolidation press with a tight-fitting loading platen was used to consolidate the sample.

Consolidation took place over a 10 d period, including 1 d of swelling. McNamara (2001) found that after approximately 1 week the vertical movement of the ram was negligible, for a sample of similar height.

A maximum consolidation pressure of 500 kPa followed by swelling to 250 kPa resulted in a sample at 50g with an overconsolidation ratio (OCR) variation with depth. The variation of K_0 with depth was calculated using Equation 1 after Mayne and Kulhawy (1982)

$$1. \quad K_0 = (1 - \sin\phi')\mathrm{OCR}^{\sin\phi'}$$

where ϕ' is taken as 23°. The consequent theoretical vertical and horizontal total and effective stresses and OCR with depth are shown in Figures 1(a) and 1(b). The undrained shear strength was measured in each test and is presented in Figure 2. Both in-flight T-bar measurements and post-flight shear vane readings were taken. The shear vane results show a more linear increase in strength with depth and have been used for the numerical analysis of test results.

5. Apparatus

Several pieces of apparatus were designed and developed as part of the project. These included pile cutting tools, guides, jigs and pile loading equipment.

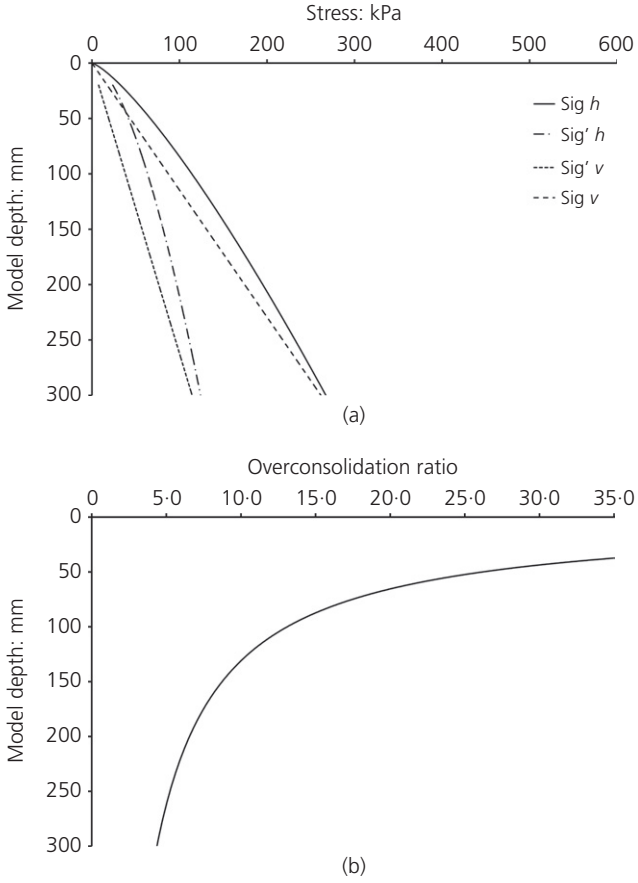

Figure 1. (a) Variation of soil sample in situ stress with depth. (b) Variation of soil sample OCR with depth

5.1 Pile cutting tools

The piles used in the tests were 16 mm in diameter by 180 mm long; at 50***g*** this scales to an 800 mm diameter by 9 m long pile. For the ribbed piles the shaft diameter remained constant at 16 mm, the ribs protruded radially outwards. For all tests the rib outstand and height remained constant at 1·5 mm.

The plain piles were cut using a hypodermic tube with an external diameter of 16 mm and wall thickness of 0·5 mm. The hypodermic tube was mounted onto a knurled brass handle to allow for easy cutting.

The pile cutting tube was guided using collars to maintain position and verticality. Several steps were taken to reduce the friction on the cutter and minimise soil disturbance within the pile bore. These included the use of a spray lubricant inside the pile bore to allow the cut soil to move more freely inside the tube, as well as a sharpened edge on the tool. Moreover, the boring of the pile took place in three equal stages.

The ribbed piles were formed by initially boring a hole in the clay using the plain pile cutter. A specifically designed tool was then placed into the bore and used to profile the ribs (as shown in Figure 3). The tool was inserted with the profiling teeth retracted; at this point the teeth were opened such that they projected outside the 16 mm bore and the entire tool was rotated. The teeth were then retracted, forcing any spoil into the tool. The various types of pile tested are shown in Figure 4.

The piles were cast using a polyurethane resin called Sika Biresein G27, which is a two-part 'fast-cast' resin used commercially for complex and rotational moulding. A ratio of 1:1:3 was used, where the larger part represents an aluminium trihydrate filler chosen for the main testing series. This mix was shown to have a density of around 1800 kg/m^3 and a pot life of 3·5 min. Figure 5 shows the pile cutting and casting arrangement. Figure 6 shows some of the exhumed piles.

5.2 Sealing of the model

The top surface of the clay was sealed with a product known commercially as PlastiDip, a multipurpose synthetic rubber coating. The spray on membrane adheres to the top of the clay and once dried (3–4 min) can be cut with a scalpel. The cured membrane has been measured to be 400 μm thick. The PlastiDip was removed at both the pile test and T-bar sites, so as not to influence the test. A bead of silicone grease around the edge of the tub ensured the sample remained sealed during any swelling of the clay.

6. Centrifuge testing procedure

The Geotechnical Engineering Research Group at City University makes use of an Acutronic 661 beam centrifuge, described in detail by Schofield and Taylor (1988).

The model was installed into the centrifuge once the piles had been cut and cast and the apparatus mounted. The water level was maintained in-flight by a standpipe. The model was left for 50 h at high ***g*** to allow the pore water pressures to reach equilibrium. Pore pressure equalisation was verified by real-time monitoring of the installed pore pressure transducers (PPTs). Once fully hydrostatic pore pressures were established, the testing of the piles could commence.

The piles were loaded simultaneously at a rate of 0·25 mm/min for at least 12 min or 3 mm of settlement. This is comparable to constant rate of penetration tests conducted at prototype scale.

7. Test analysis

Results obtained from each pile load test have been analysed using several techniques to better define the behaviour of the test pile and allow for comparison between plain shafted piles.

The first technique used was to normalise the load–settlement behaviour of a ribbed pile against the plain pile used in the same test. This allowed for any inconsistencies in the soil sample to be accounted for, including any variation in

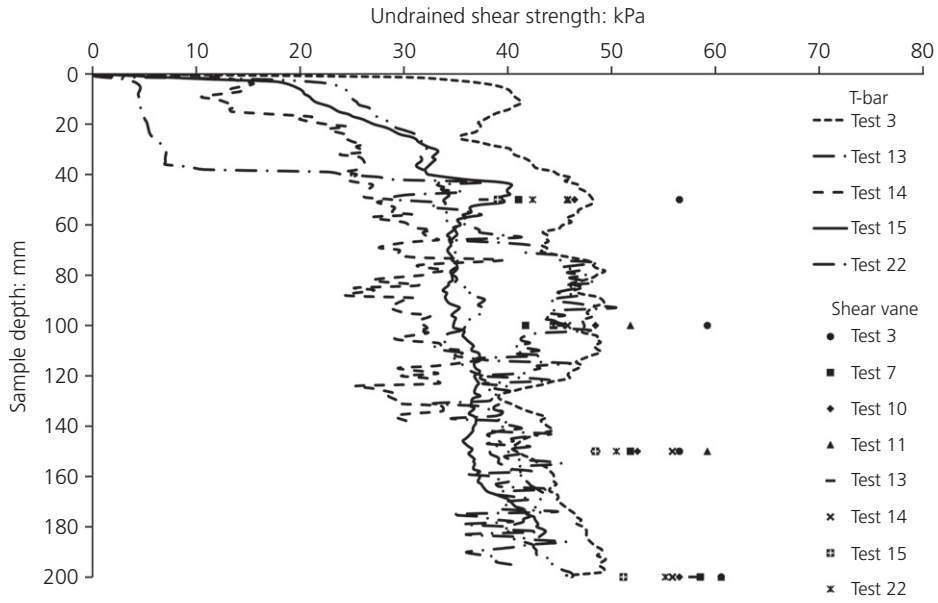

Figure 2. T-bar obtained undrained shear strength with depth

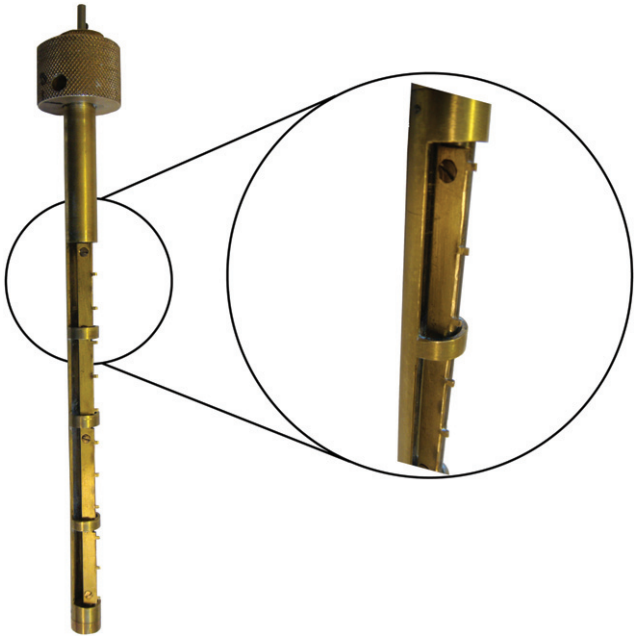

Figure 3. Rib cutting tool

undrained shear strength profile. It can be assumed that two identical piles in the same soil sample, subject to the same load, will respond in the same way. It follows therefore that the behaviour of a ribbed pile can be compared to that of the plain pile to ascertain any relative improvement in performance.

Figure 7 shows the normalised load–settlement curves for each test. In each case the ribbed pile load data have been

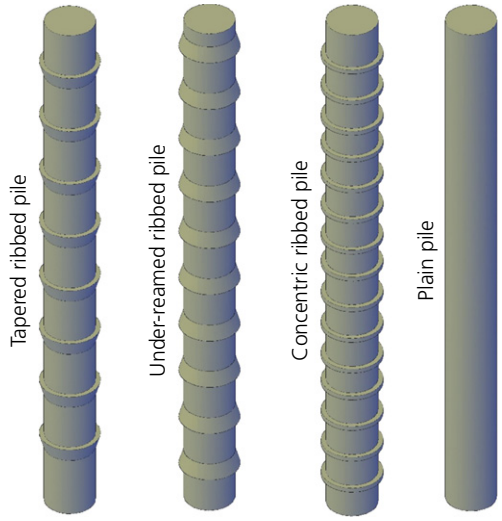

Figure 4. Pile types

normalised against the load data of the plain pile used in the same test.

To allow for comparison Figure 7 has been broken down into several simpler graphs shown in Figures 8 and 9. The 10 mm spacing (at model scale) has been shown to be the most effective in increasing the ultimate capacity of the pile. The normalised increase in capacity decreased as the rib spacing increased.

The tapered rib pile was also very effective and almost matched the normalised load of the 10 mm spaced ribs (Figure 7). However, this increase in normalised load was only

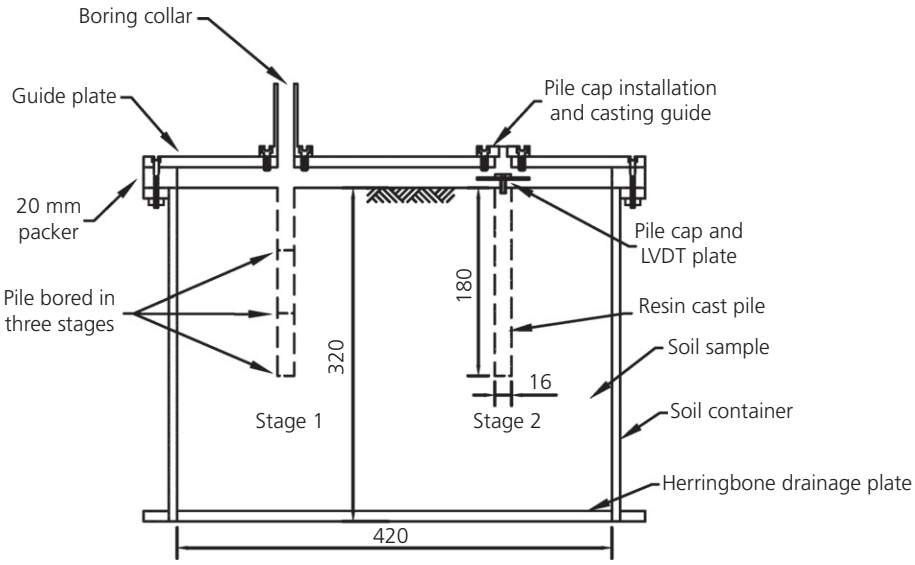

Figure 5. Pile cutting and casting arrangement (dimensions: mm; LVDT: linear variable differential transducer)

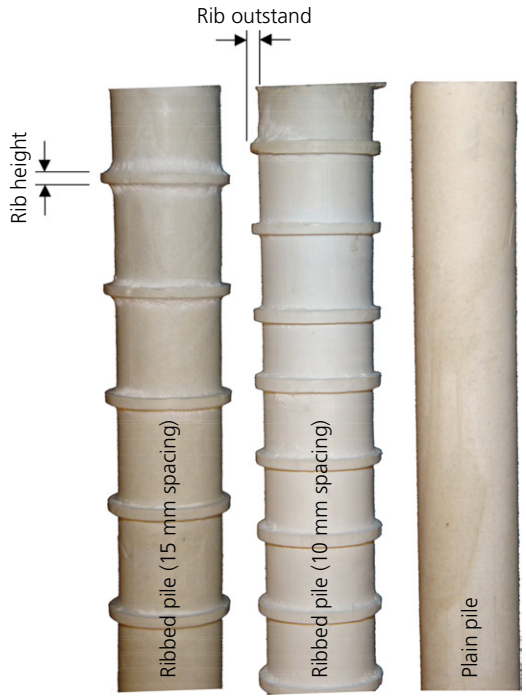

Figure 6. Photographs of exhumed piles

evident after a significant amount of initial settlement, whereas the ribbed piles showed an improvement in normalised load during the earlier stages of loading.

Figure 9 shows a normalised load–settlement curve for the 19 mm plain pile, which is a pile with a diameter equivalent to that of the outer diameter of the ribs. By comparing the 19 mm plain pile to the other normalised load–settlement curves, it can be seen that the 10 mm ribbed and the tapered rib pile out-performed a plain pile of diameter equal to the outer rib diameter.

In test 14 the behaviour of a pile in which only the bottom third was profiled using ribs at 10 mm spacing was explored. The normalised load–settlement curve (Figure 9) shows the performance of the pile was inferior when compared to the plain pile for the majority of the test; however, near the maximum settlement the ribbed pile showed a slight improvement. This suggests the additional capacity mobilised by the ribs is contributed by end bearing, which for bored cast in situ piles is usually accepted to be generated after significant vertical settlement.

By normalising the load–settlement curve in each test it is evident that the ribbed piles provided a more efficient pile, given that the normalised load at failure was higher than for a plain pile (Figure 7). However, this technique provides no insight as to how the additional capacity has been generated.

In order to better understand the behaviour of the ribbed pile, it was necessary to define the point at which each test pile had failed. Several methods were considered (Brinch Hansen, 1963; BS 8004 (BSI, 1986); Chin, 1970; Fuller and Hoy, 1970) to analyse and define the failure load of every pile tested (Table 1). A spreadsheet was set up for each failure criterion and used to calculate the failure load in an identical fashion, thus removing the variable of human interpretation. None of the failure criteria used gave an output constantly higher or

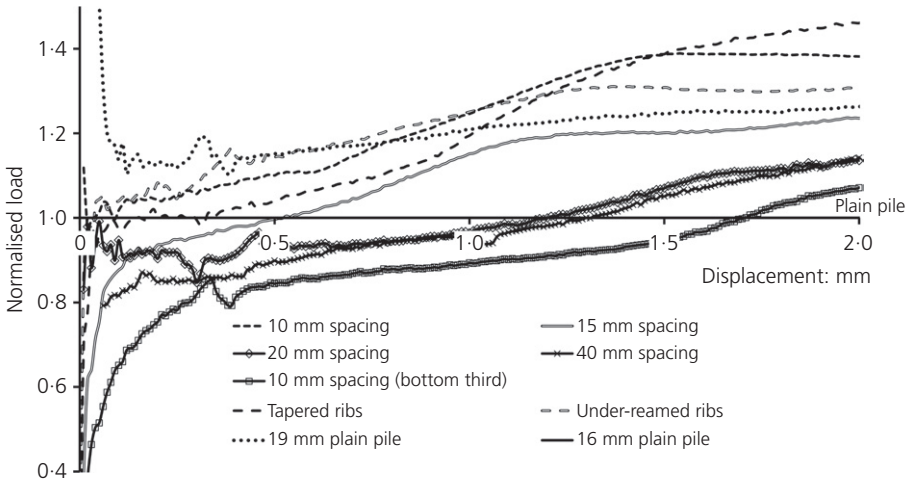

Figure 7. Normalised load–settlement curves for each test

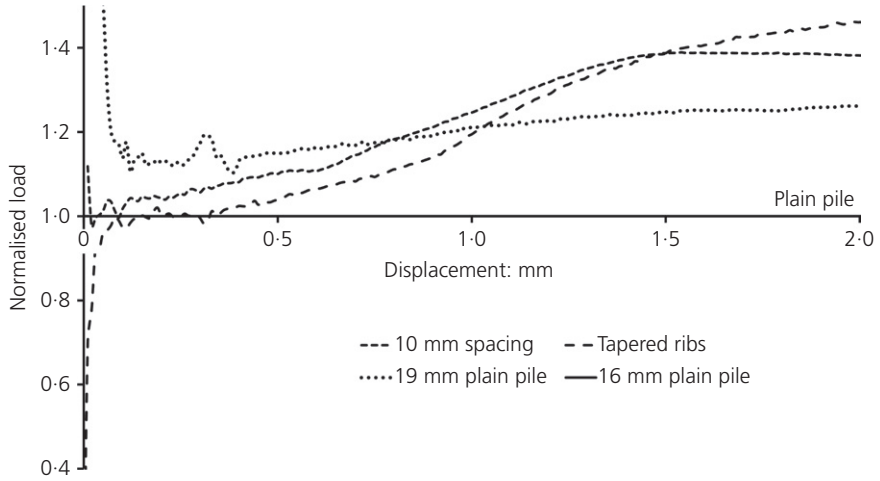

Figure 8. Normalised load–settlement curve for tapered and 10 mm concentric ribs

lower when compared to another; instead the outputs from each of the analyses were generally within 10–15%. For this reason a mean average of the four methods was used to define the failure load of the pile. The defined failure load has also been scaled up to prototype scale. Table 1 also shows the percentage improvement in capacity of the ribbed pile relative to the plain pile in the same test. This improvement in ultimate load capacity varied from a 3% to a 57% increase.

The calculated failure loads for all of the plain piles showed some variation. This can probably be attributed to inconsistencies in the soil sample, and also the type of resin used to cast the piles. It is therefore necessary to consider the plain pile used in each test when analysing the ribbed pile behaviour. In all cases the ribbed pile showed an improvement over the plain pile. The 19 mm plain pile showed a 27% increase in load capacity at failure when compared with the 16 mm plain pile.

The normalised load capacity has been plotted against the rib spacing (Figure 10). Also plotted are the plain pile normalised failure load and the 19 mm plain pile normalised failure load. The 10 mm spaced rib piles show a normalised capacity greater than a pile with an outer diameter equal to the rib diameter. The 10 mm spaced ribbed pile also showed increased capacity when compared to the 19 mm pile. The remaining ribbed piles all exhibited an improvement over the plain pile, but were out-performed by the 19 mm plain pile.

8. Pile design framework

From the analysis conducted there is a clear trend between the rib spacing and the increase in pile capacity. In order to allow

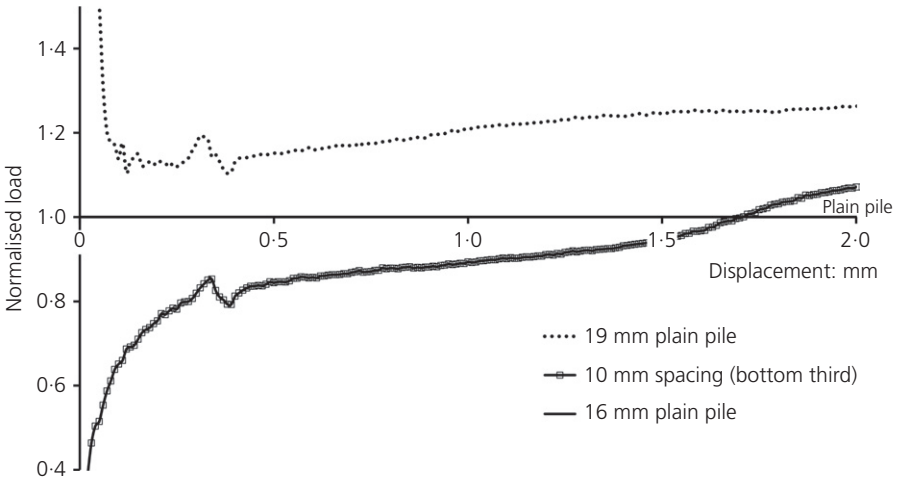

Figure 9. Normalised load–settlement curve for the bottom third ribbed pile

for design of these ribbed piles, a framework must be established.

8.1 Longitudinal cross-sectional area method

Figure 11 shows a graph of percentage capacity (when compared to the plain pile in the same test) against the percentage of sectional area (i.e. the area presented if the pile were cut in half along its length). Also on this plot is a ±10% error band. All of the tests show good correlation with the proposed best-fit line and all are approximately within the 10% error band. The best-fit line has the following equation

$$K = 0{\cdot}0445M + 95{\cdot}91 \quad (2)$$

where K is the percentage of longitudinal cross-sectional area compared to the plain pile and M is the percentage of capacity when compared to a plain pile.

With this information it is possible to predict the increase in the capacity of a ribbed piles using the longitudinal cross sectional area to an accuracy of ±10%.

If this method were to be used to design a ribbed pile it is envisaged the design engineer would first conduct a standard plain pile calculation. A decision would then be made on what additional capacity is required. Equation 2 would then be used to calculate the additional cross-sectional area required. A rib size and spacing could then be designed to suit the required increase in longitudinal cross-sectional area. This would assume square ribs evenly spaced, as this is the range of geometries tested.

This method requires refinement because a larger diameter plain pile, for example a 19 mm diameter pile, will have an increase in cross-sectional area of 118·75%. Analysis of test 11 suggested such a pile would have an increase in capacity of 127% when compared to a 16 mm diameter pile. If this data point were plotted on Figure 11, it could be seen that Equation 2 does not apply. This is owing to the 19 mm diameter pile being thought of as a 16 mm diameter ribbed pile with effectively zero rib spacing. The point at which a ribbed pile becomes a plain pile with diameter equivalent to the outer rib diameter is not clear.

8.2 Detailed design method

The longitudinal sectional area method described above is an empirical method for geotechnical design of ribbed piles. A more detailed design method would be required before ribbed piles could be justified for use in industry.

8.3 The theoretical capacity of a plain pile

In the first instance it was necessary to calculate the theoretical capacity of the plain pile in each test. This would allow for derivation of the adhesion factor which would be required in any ribbed pile design.

The theoretical ultimate capacity of a plain pile can be calculated using the following equation

$$Q_u = Q_s + Q_b - W \quad (3)$$

where Q_u is the ultimate loading capacity of the pile; Q_s is the ultimate skin friction; Q_b is the ultimate base resistance; and W is the pile self-weight.

The undrained shear strength profile with depth varied for each test. For the purpose of theoretically calculating the capacity of the pile, a best-fit line was applied to the measured

Test ID	Pile description	Chin (1970) failure load: N	BS 8004 (BSI, 1986) failure load: N	Fuller and Hoy (1970) failure load: N	Brinch Hansen (1963) failure load: N	Average failure load: N	Failure load at prototype scale: kN	Capacity increase: %
22	Under-reamed rib	597	532	547	547	556	1389	41
	Plain pile	400	409	379	391	395	987	
15	Tapered rib	525	505	501	497	507	1268	40
	Plain pile	345	359	353	389	361	904	
14	Bottom third ribbed	443	401	411	405	415	1037	3
	Plain pile	389	416	372	428	401	1003	
13	40 mm spacing	523	449	485	451	477	1193	16
	Plain pile	401	419	390	440	413	1032	
11	19 mm plain pile	613	546	545	551	564	1049	27
	Plain pile	470	437	423	441	443	1107	
10	20 mm spacing	514	459	485	475	483	1208	20
	Plain pile	383	417	382	433	404	1010	
7	15 mm spacing	565	467	510	508	512	1281	36
	Plain pile	389	388	375	357	377	943	
3	10 mm spacing	967	845	823	845	870	2175	40
	Plain pile	629	609	615	632	621	1554	

Table 1. Results of test pile failure analysis

post-test shear vane readings from each test (Figure 2). From this best-fit line it was possible to estimate the undrained shear strength at any depth in any particular test.

8.3.1 End bearing capacity

The plastic failure envelope presented by Meyerhof (1951) shown in Figure 12 consists of two zones. Zone ABC remains elastic and acts as part of the foundation. Zone ACD is that of radial shear. The end bearing capacity of a piled foundation can therefore be calculated using the following equation

$$4. \quad Q_b = A_b\left(N_c S_{u(base)} + \gamma L\right)$$

where A_b is the cross-sectional area of the pile base; $S_{u(base)}$ is the undrained shear strength at the pile base; N_c is the bearing capacity factor; γ is the unit weight of the soil; and L is the pile length.

Fleming *et al.* (1992) suggested that linear interpolation should be made between $N_c = 6$ for the case of the pile just reaching the bearing stratum and up to $N_c = 9$ where the pile penetrates a stiff layer by three diameters or more. As this study is concerned with piles installed in a single sample of soil, the bearing capacity factor for every test pile can be taken as 6.

Using the undrained shear strength profile obtained from the T-bar, where available, the shear vane readings and an N_c value of 6, it was possible to calculate the theoretical bearing capacity of the plain pile for every test.

8.3.2 Shaft capacity

From the various failure analyses conducted for each test the ultimate failure load of every plain pile was identified. The shaft capacity of the pile is computed from Equation 3, using the mean values of Q_u in Table 1, less the value of Q_b from Equation 4 and accounting for the pile weight, W. The adhesion achieved by each plain pile could then also be calculated using Equation 5.

$$5. \quad Q_s = A_s \alpha S_{u(avg)}$$

where Q_s is the ultimate skin friction; A_s is the shaft area; α is the adhesion factor; and $S_{u(avg)}$ is the average undrained shear strength of the clay along the pile shaft.

The value of α achieved in all tests varied from 0·67 to 1. This is within the expected range for the pile material and model preparation method. The back-calculated α for each plain pile is shown in Table 2.

8.4 Ribbed pile capacity

Traditional pile capacity calculations are categorised into two constitutive parts, namely the base resistance and shaft resistance. This is because these two components cause very different failure mechanisms within the soil, and therefore generate the resistance in a different way. A similar approach has been

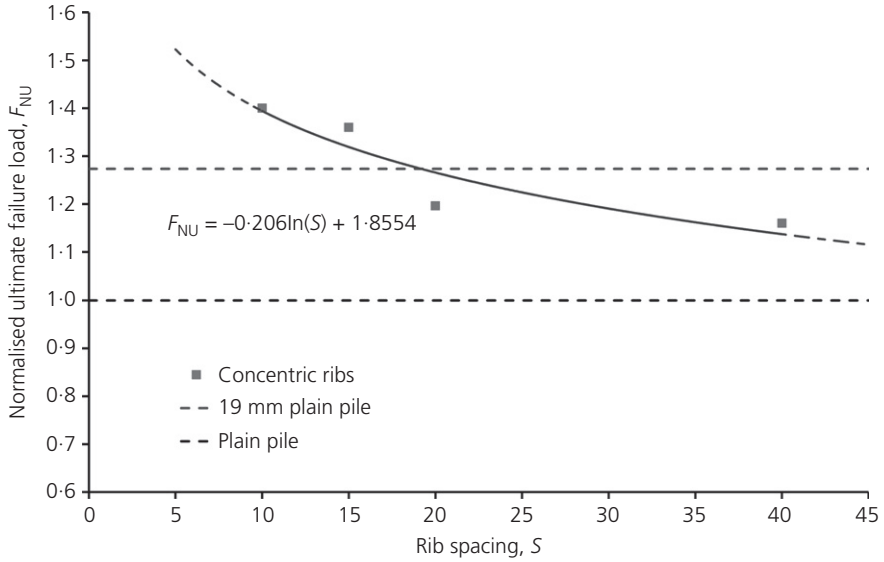

Figure 10. Normalised ultimate failure load plotted against rib spacing

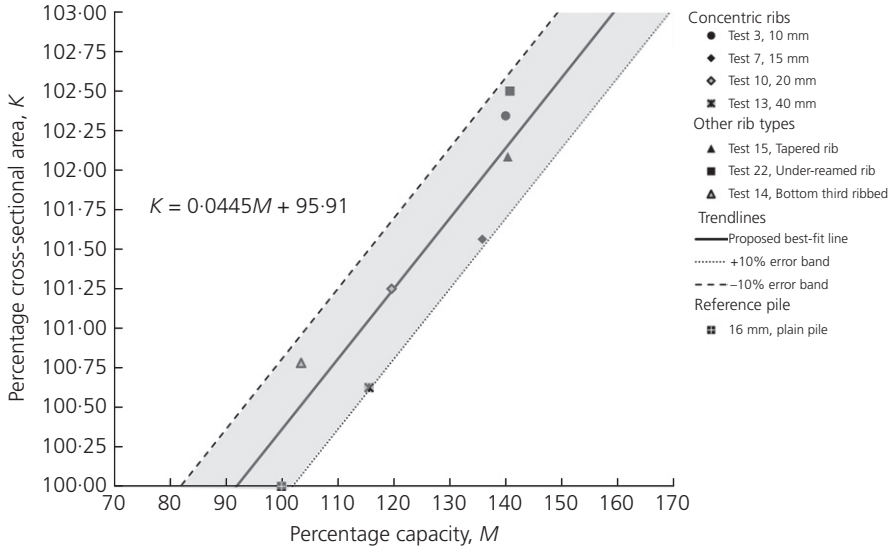

Note: Percentages are compared to the reference (16 mm) pile

Figure 11. Percentage increase in pile capacity plotted against increase in cross-sectional area

adopted to allow for the design of ribbed pile foundations. Equation 3 can be rewritten to include the additional capacity generated by the pile ribs

$$6. \quad Q_u = \sum Q_s + Q_b + \sum Q_{rs} + \sum Q_{rb} - W$$

where Q_u is the ultimate loading capacity of the pile; Q_s is the ultimate skin friction along the plain shaft; Q_b is the ultimate base resistance; Q_{rs} is the ultimate skin friction along the rib shaft; Q_{rb} is the ultimate base resistance from each rib; and W is the pile self-weight.

8.4.1 Base and shaft capacity of ribbed piles

The base resistance for each rib was calculated using the same method as for the base of a plain pile. The shaft capacity was calculated according to the space between two adjacent ribs. However, the average shear strength was calculated across the distance between each set of adjacent ribs as opposed to the

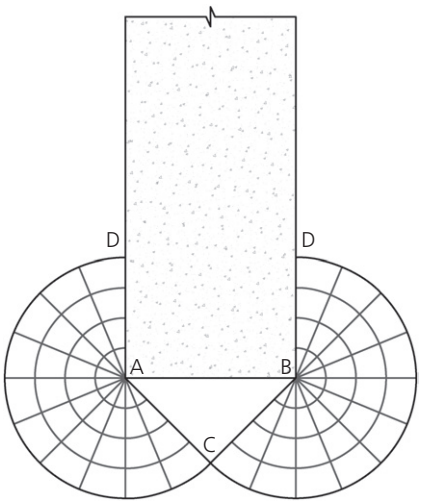

Figure 12. Meyerhof (1951) plastic failure envelope for pile end bearing

Test ID	Test type	Rib spacing	Alpha
22	Under-reamed	15	0·94
15	Tapered	15	1
14	Concentric – bottom third	10	0·78
13	Concentric	40	0·95
10	Concentric	20	0·77
7	Concentric	15	0·78
3	Concentric	10	1

Table 2. Back calculated alpha for plain piles

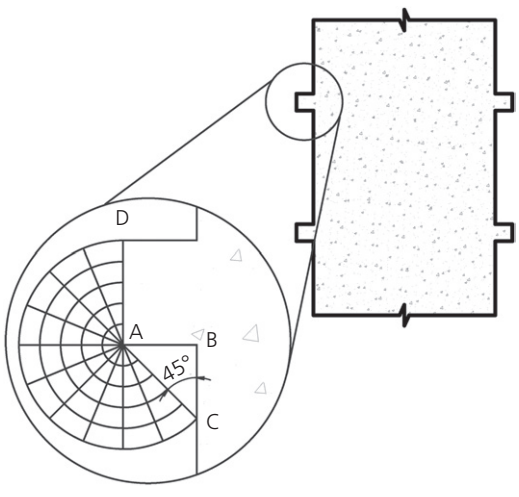

Figure 13. Plastic failure envelope for pile rib in end bearing

entire length of the pile. The adhesion factor used in this calculation was the same as that calculated for the plain pile in that test. The sum of these individual shaft capacities were then used, to give a total shaft capacity (Q_s). This design method is broadly similar to that routinely used for steel screw piles.

8.4.2 Rib base and rib shaft capacity of ribbed piles

The plastic failure envelope of the rib base is likely to be similar to the Meyerhof (1951) plastic failure envelope. The proposed plastic failure envelope for a pile rib is shown in Figure 13. An angle of 45° has been used for the undrained plastic failure zone. The plug underneath each rib defined by the triangle ABC remains elastic and fails as part of the foundation. The existence of this intact plug of soil has been verified visually during deconstruction of each test. This small area must therefore not be included in the shaft shear capacity calculation. The area ACD is that of radial shear.

The shaft capacity for each rib was calculated using the standard method, as the failure mechanism is likely to be the same as the shaft of a plain pile. The adhesion factor used was the same as that for the plain pile in the corresponding reference test and the outer rib diameter was taken as the clay–pile shear interface.

8.5 Comparison of framework to actual test data

The various theoretical pile capacity calculation techniques described above were applied to every pile tested. Each pile was surveyed and weighed post-test to confirm the physical properties. Allowances were made in the theoretical calculations for imperfections to the pile where these existed. Table 3 summarises the theoretical capacity as calculated by the above methods. This has also been compared to the actual test capacity of the pile. The difference between the actual capacity and the theoretical capacity for ribbed piles is within ±8%. This is clear evidence that, for the range of geometries tested in overconsolidated clay, the framework set out above is an effective solution for the theoretical calculation of ultimate capacity of a ribbed pile.

8.6 Structural capacity of pile rib

The addition of ribs has been shown to increase the ultimate capacity of a bored pile in the model scale, with a two-part resin used as the construction material. However, if this rib is unable to withstand the forces applied at prototype scale, the technique is of little use. The most likely failure mode is in shear between a concrete rib and the pile shaft. The rib dimensions used in this project scale to 75 mm square at prototype scale. Assuming the pile is constructed from C40 concrete and the rib remains unreinforced, it can be shown that for the given dimensions the applied shear force is around a quarter of the available shear resistance, and hence well within acceptable limits.

Test no.	Rib type	Q_b: N	ΣQ_{rb}: N	ΣQ_s: N	ΣQ_{rs}: N	Theoretical capacity: N	Test capacity: N	Percentage difference: %	Equivalent plain pile diameter: m
22	20 mm (under-reamed)	144	392	546	264	1346	1389	−3·26	1·07
15	20 mm (tapered)	152	422	595	209	1378	1268	7·95	1·01
14	10 mm (bottom third)	187	329	561	46	1123	1037	7·65	0·82
13	40 mm	164	215	786	39	1204	1193	0·97	0·91
10	20 mm	165	333	694	42	1234	1208	2·14	0·93
7	15 mm	168	533	597	76	1374	1281	6·81	1·03
3	10 mm	184	1039	851	188	2262	2175	3·81	1·13

Table 3. Summary of theoretically calculated and test rib pile capacity

9. Limitations and implications of results

As with all modelling techniques, centrifuge modelling has some level of idealisation which may not be completely representative of prototype situations. The behaviour of soil is dependent on its stress state, stress history and permeability. For centrifuge modelling, speswhite kaolin clay was used, primarily for its high permeability compared to other clays. The high permeability allows the time for model preparation and consolidation to be considerably reduced relative to prototype soils.

The piles were installed at 1g on the laboratory floor rather than a high-g environment. At the time of pile installation the pore pressures in the sample were likely to be in suction, as the sample had recently been removed from the consolidation press. This is clearly not representative of the prototype scale. Moreover, there were no attempts made to install the piles in flight, and thus there is no way of quantifying the effect of 1g pile installation. However, the effect of installation is not believed to be significant, primarily as all the tests were subject to the same phenomena and hence remained internally consistent. Second, the soil model post-pile installation was subjected to a high gravity field for over 2 d, allowing the soil immediately adjacent to the pile to consolidate around the pile. The resin used to cast the piles was also an idealisation, the elastic shortening of the resin is not the same as that of concrete; however, since both piles within each test were made of the same material, the elastic shortening of each pile is comparable. The adhesion between the resin and kaolin clay sample may not be representative of the adhesion between concrete and a heavily overconsolidated clay, for example. However, every pile tested was subject to both of these idealisations and hence the test series remains internally consistent, although this poses some difficulty when making comparisons to prototype scale tests.

The ribbed bored pile provides several benefits over a conventional bored pile. A smaller diameter and shallower piled foundation would translate to less spoil removal and less concrete use, resulting in a more environmentally friendly foundation, adding to the green credentials of any project. Furthermore, smaller diameter and shallower piled foundations will allow for installation in between other new or existing piles and perhaps even in low-headroom applications.

The use of ribbed piles is a clear advancement in piling technology and provides another option to contractors and designers when building foundations for structures. For the technique to become widely used, the tooling and machinery must be developed, and manufactured, such that the additional effort and cost required to install the pile ribs is sufficiently reduced in comparison to the cost of boring a deeper and or wider pile.

10. Recommendations for further research

A significant programme of field testing is required to support the theories presented here. This should also be correlated with numerical analyses to provide much-needed additional data to enable predictions of ribbed pile ultimate capacities to be made with more confidence.

REFERENCES

Brinch Hansen J (1963) Discussion, 'Hyperbolic stress–strain response. Cohesive soils'. *Journal of the Soil Mechanics and Foundation Division, ASCE* **89(SM4)**: 241–242.

BSI (1986) BS 8004: British standard code of practice for foundations. BSI, Milton Keynes, UK.

Chapman T, Marsh B and Foster A (2001) Foundations for the future. *Proceedings of the Institution of Civil Engineers – Civil Engineering* **144(1)**: 36–41.

Chin FK (1970) Estimation of the ultimate load of piles not carried to failure. *Proceedings of the 2nd Southeast Asian Conference on Soil Engineering, Singapore*, pp. 81–90.

Craig WH (1995) Geotechnical centrifuges: past, present and future. In *Geotechnical Centrifuge Technology* (Taylor RN (ed.)). Blackie Academic and Professional, Glasgow, UK, ch. 1, pp. 1–19.

Fleming WGK, Weltman AJ, Randolph HF and Elson WK (1992) *Piling Engineering*, 2nd edn. Blackie, Glasgow, UK.

Fuller FM and Hoy HE (1970) *Pile Load Tests Including Quick Load Test Method, Conventional Methods, and Interpretations*. Highway Research Board, Washington, DC, USA, Research Record 333, pp. 74–86.

Ground Engineering (2003) Getting to grips with friction. *Ground Engineering, Magazine of the British Geotechnical Association* **26**: 20–21.

Mayne PW and Kulhawy FH (1982) K_0–OCR relationship in soil. *Proceeding of ASCE, Journal of the Geotechnical Engineering Division* **108(6)**: 851–872.

McNamara AM (2001) *Influence of Heave Reducing Piles on Ground Movements Around Excavations*. PhD thesis, City University, London, UK.

Meyerhof GG (1951) The ultimate bearing capacity of foundations. *Géotechnique* **2(4)**: 301–332.

Qerimi LB (2009) *Geotechnical Centrifuge Model Testing for Pile Foundation Re-Use*. PhD thesis, City University, London, UK.

Schofield AN and Taylor RN (1988) Development of standard geotechnical centrifuge operations. In *Centrifuge 88* (Corte JF (ed.)). Balkema, Rotterdam, the Netherlands, pp. 29–32.